New ultraviolet radiometry beamline at the Synchrotron Ultraviolet Radiation Facility at NIST

P.-S. Shaw, K. R. Lykke, R. Gupta, T. R. O'Brian, U. Arp, H. H. White, T. B. Lucatorto, J. L. Dehmer and A. C. Parr

Abstract. We have constructed a new ultraviolet (UV) radiometry facility at the Synchrotron Ultraviolet Radiation Facility (SURF II) at the National Institute of Standards and Technology (NIST). The facility combines a high-throughput normal-incidence monochromator with an absolute cryogenic radiometer (ACR) optimized for UV measurements to provide absolute detector-based radiometric calibrations in the spectral range 125 nm to approximately 320 nm. The system can be configured for spectroradiometric calibration of photodetectors with completely automated mapping of detector spatial and angular responsivity. The facility can easily be adapted for other spectroradiometric measurements including transmittance and reflectance and the spectral range can be extended to about 50 nm.

1. Introduction

A synchrotron-radiation source provides a broadband, continuous spectrum that ranges from infrared to x-ray wavelengths with high brightness and low beam divergence [1, 2]. In addition, the properties of the synchrotron radiation (such as spectral distribution, polarization, and angular divergence) can be accurately calculated from the machine parameters. These characteristics make synchrotron radiation much superior to conventional laboratory light sources for UV, vacuum ultraviolet (VUV), and x-ray radiometry. In response to a demand from industry for improved radiometric accuracy in the UV and VUV regions of the spectrum [3], we at NIST have established a new radiometric-beamline facility at SURF II. The key new element in this facility is the ACR, a type of absolute detector that has previously been responsible for a remarkable improvement in accuracy in visible and near-infrared (NIR) detector calibrations at NIST.

The ACR measures the incident radiant power with high accuracy by using electrical substitution [4]. For example, at NIST, the High Accuracy Cryogenic Radiometer (HACR) [5] is an ACR primary detector standard that uses intensity-stabilized laser beams for detector calibration in the visible and NIR spectral ranges. The achieved relative standard uncertainty of the spectral responsivity is less than 0.03 %. The extension of an ACR for use in the UV, VUV, and soft-x-ray spectral ranges with synchrotron radiation was first demonstrated [6, 7] by the Physikalisch-Technische Bundesanstalt (PTB) at the Berlin electron-storage ring (BESSY). The relative standard uncertainty achieved is below 1 % for most of the spectral range [8].

Previous to the present work, two standards were used for detector calibration at SURF II: a rare-gas double-ionization chamber as a primary detector standard [9] and the SURF II storage ring as a primary source standard [2, 10]. For the new radiometry beamline, the ACR is used as a primary detector standard for the spectral range 125 nm to 320 nm [2]. This range was selected to complement the NIST UV Spectral Comparator Facility (UVSCF) [11, 12], which calibrates detectors using an argon mini-arc lamp and monochromator source. The spectral range of the UVSCF is limited in the UV to $\lambda > 200$ nm. The new radiometry beamline extends beyond the spectral range of the UVSCF and includes wavelengths such as 193 nm and 157 nm excimer laser lines that are particularly interesting for semiconductor photolithography.

2. Beamline description

The new radiometry facility was constructed on beamline 4 at SURF II. The schematic of the beamline components is shown in Figure 1. A 2 m normal-incidence monochromator was used to disperse the synchrotron radiation from the storage ring [13]. For the work reported in this paper, a 600 line/mm grating blazed at 200 nm was used in the monochromator. Synchrotron radiation emitted from the electron-storage ring is imaged on to the entrance slit of the 2 m monochromator by two grazing-incidence (80°) fused-

P.-S. Shaw, K. R. Lykke, R. Gupta, T. R. O'Brian, U. Arp, H. H. White, T. B. Lucatorto, J. L. Dehmer and A. C. Parr: National Institute of Standards and Technology, Gaithersburg, MD 20899, USA.

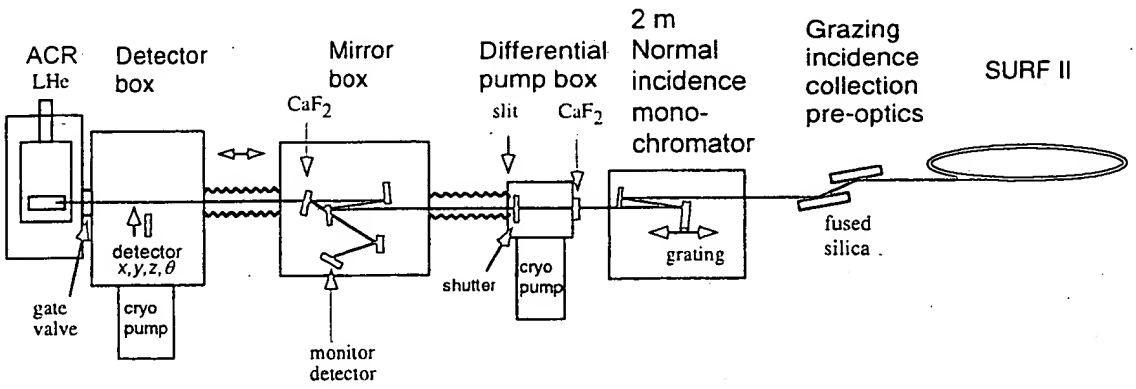

Figure 1. Schematic diagram of beamline 4 on SURF II. A fused-silica filter can be inserted into the beam near the shutter to suppress higher orders from the monochromator.

silica mirrors, one plane and the other toroidal [14]. The exit slit of the monochromator comprises two sets of adjustable slits to control the resolution and the size of the exit beam in both horizontal and vertical directions. For a 1 mm by 1 mm beam, the resolution is 0.7 nm at 200 nm. Immediately before the exit slit, a CaF_2 window is used to isolate the vacuum of the monochromator and the electron-storage ring from the vacuum of the rest of the beamline. This reduces the vacuum requirement for the vacuum chamber that houses the detectors for calibration and shortens the turnover time for detector calibration. To open a non-isolated beamline to the electron ring at SURF II, the vacuum requirements are very strict and turnover time can be greater than one week. By isolating the detector chamber from the ring with the CaF_2 window, turnover time is on the order of a few minutes. The CaF_2 window also limits the spectral range to $\lambda > 120$ nm. For future calibration below 120 nm, this window will be removed.

To characterize the exit beam from the monochromator, a CCD camera was used to measure the beam divergence and the effect of astigmatism. The measured beam divergence is about 1° in the vertical direction and 2° in the horizontal direction. The output power of the synchrotron radiation transmitted by the monochromator was also measured with the ACR. A typical result is shown in Figure 2 with the SURF electron beam operated at an energy of 256 MeV and a current of 90 mA. Note that for wavelengths longer than 240 nm a fused-silica filter was inserted into the beam to suppress higher-diffraction-order contributions. In addition, the spectral purity of the beam was studied by measuring the scattered light emanating from the slit below the fused-silica cutoff.

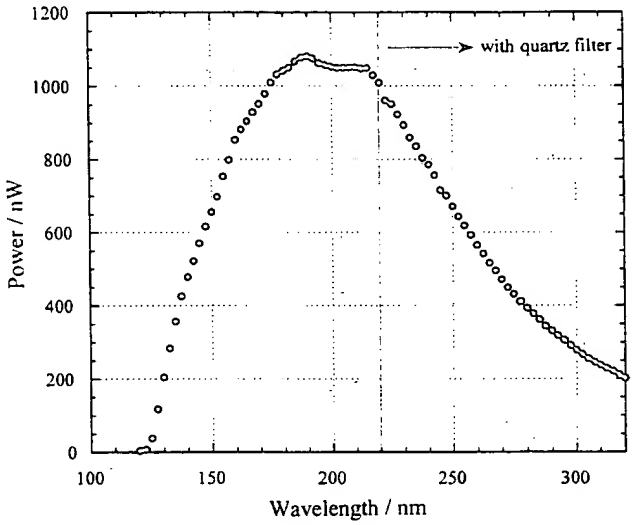

Figure 2. Power output of beamline 4 at SURF II with a beam current of 90 mA and a 3 mm × 3 mm slit (approximately 2 nm resolution).

3. Detector endstation

The endstation of the new radiometry beamline consists of three parts: the refocusing optics, the detector box, and the ACR (see Figure 1). Refocusing optics are used to image the light from the monochromator exit slit on to the test detector or the ACR (one-to-one imaging). There are two mirrors, one plane and the other spherical, aligned at near-normal incidence to the synchrotron radiation. A small portion of the beam is reflected by the CaF_2 beam splitter on to a monitor photodiode, which is used to normalize either the signal from the detector under test or the signal from the ACR. This monitor is important since it makes detector calibration insensitive to the gradual decay of the electron beam in the storage ring and also to any fluctuations caused by the monochromator system.

The detector box is connected to the mirror box by a flexible vacuum bellows. The detector under test is mounted on in-vacuum translation stages that can move linearly in two orthogonal directions in the plane normal to the synchrotron-radiation beam. The detector mount also has a rotary motion about the vertical direction to adjust the incidence angle of light on the detector. All detector motions are controlled by computer. The x-y translations relocate the detector in and out of the optical path so that the synchrotron radiation can illuminate the detector and ACR sequentially. In addition, the linear

movements can also be used to study the uniformity of the detector responsivity. An additional photodiode with a small aperture can also be mounted alongside the detector to study the synchrotron-radiation beam profile.

Downstream, the ACR is connected directly to the detector chamber with a gate valve. While the synchrotron-radiation beam can impinge on either the ACR or the detector (depending on the position of the detector), the physical separation between the ACR and detector means that the synchrotron-radiation beam divergence creates some difference in beam profiles as viewed by the ACR or the detector. Too much divergence can cause the beam to overfill the cavity and cause an error in the measured radiant power. To ensure that the detector and the ACR can both be brought to the focal plane, another linear-motion stage is used to move the detector chamber and the ACR together in the direction of the synchrotron-radiation beam. This movement can bring either detector into the focal plane. When the photodiode measurement is complete, the in-vacuum (x) stage moves the detector out of the beam path to allow the beam into the ACR. At the same time, both the detector chamber and the ACR move towards the storage ring and so the focusing point is near the entrance of the ACR cavity. All the linear stages are controlled by the same computer and all movements are automated.

4. Absolute cryogenic radiometers

Absolute cryogenic radiometers (or electrical-substitution radiometers) have now been in use for over ten years [4]. The idea is that electrical power to heat a cavity and optical power to heat the cavity to the same temperature are fundamentally the same. The temperature of a receiver cavity is actively stabilized by electrical power at some temperature (just above 4.2 K) and this cavity has a thermal link to an actively stabilized heat sink connected to a liquid-helium-cooled Dewar. The cavity is operated at nominally 4.2 K to decrease the heat capacity and increase the thermal conductivity to allow for a rapid response. The small cavity (8 mm diameter coated with chromium oxide for UV absorptivity) has a thermal responsivity of 3.2 mK/μW with a time constant of a few seconds and a noise floor of about 2 nW.

The ACR was first compared with the NIST HACR by using a trap transfer detector that had been previously calibrated by the HACR. To achieve uncertainties that are low relative to the noise floor of the ACR (the uncertainties will be discussed in a future publication), we used an intensity-stabilized He-Ne laser at 632.8 nm to irradiate alternately the trap detector, then the ACR. Figure 3 shows a time scan of the trap versus beamline 4 of the ACR. The measured value for the ACR agreed to within 0.1 % of the HACR value.

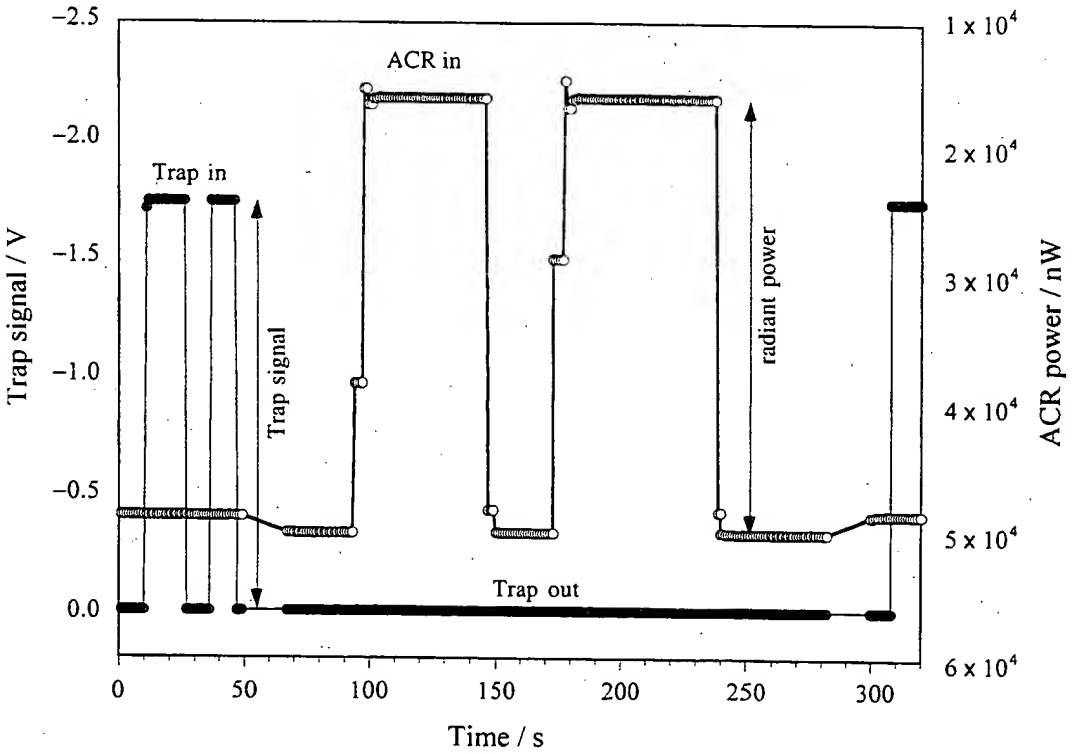

Figure 3. Comparison of the ACR at SURF II with the HACR using a transfer standard (trap detector) at 632.8 nm (He-Ne wavelength). The apparent background for the ACR changes because the ACR views either the back of the trap (for the trap reading), or the proper background that views the beamline.

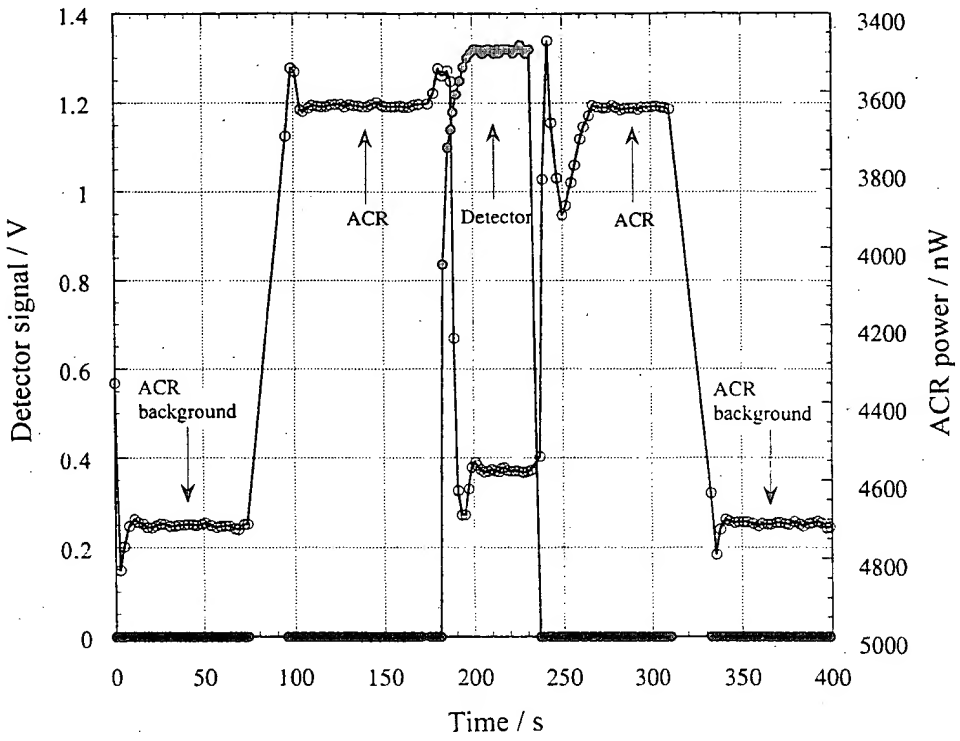

Figure 4. Graph showing the data-collection process. With the ACR in place and the wavelength of the monochromator set, the ACR background is taken (shutter closed), then the shutter is opened to obtain a power reading. This is followed by measurements of the response of the test detector, a repeat of the ACR response (this and the earlier measurement give the source power drift), and another background reading. After this, the wavelength is changed and the process is repeated.

5. Detector calibration

This beamline is used for measurements of the responsivity and the spatial uniformity of the responsivity of detectors. In a standard detector calibration, the detector is mounted in the detector chamber and the chamber is evacuated. The synchrotron radiation is then allowed to propagate to the detector. The detector is scanned in the plane normal to the light beam, and the signal from the detector is recorded by computer. With the measured detector spatial response distribution, the quality of the detector can be assessed, and a suitable position can be chosen for further responsivity study.

The procedure for responsivity measurement is demonstrated in Figure 4. To start, the detector is moved out of the beam path and the ACR moved into the focal plane. The ACR first measures the background signal by closing the shutter and then measures the synchrotron radiation by opening the shutter. After the data from the ACR are recorded, the detector is moved into the beam path at the focal plane and positioned such that the synchrotron radiation strikes the detector at the specific point selected from the uniformity measurement. The computer then collects the detector signal with the synchrotron radiation (a background is obtained while taking the ACR reading). Next, the detector is again moved out of the beam path and the ACR moved into the focal point. ACR data are again collected with and without the synchrotron radiation. From this cycle of operations, the responsivity of the detector at the particular wavelength can be determined. Simultaneously, the monitor-diode signal is collected during the whole measurement procedure. The same procedure is used at other wavelengths to generate a calibration curve for the detector.

An alternative and faster method for detector calibration is to use the signal of the monitor diode directly to determine the absolute power of the incident beam. The ratio of the signal of the monitor diode to that of the actual radiant power is determined in a separate measurement with the ACR. Once the signal of the monitor diode is correlated with the radiant power, the responsivity can be calculated from measurements of the detector and the monitor diode only.

Several different types of UV detector were calibrated using the new radiometry beamline. These include: Hamamatsu 5227, IRD UVG (nitrided oxide/Si), UDT UV, GaP, GaN, GaAsP, PtSi [15], and diamond photoconductive.[1] Figure 5 gives a representative sampling of some of these calibrations between 125 nm and 320 nm.

1. Certain commercial equipment, instruments, or materials are identified in this paper to foster understanding. Such identification does not imply recommendation or endorsement by the National Institute of Standards and Technology, nor does it imply that the materials or equipment identified are necessarily the best available for the purpose.

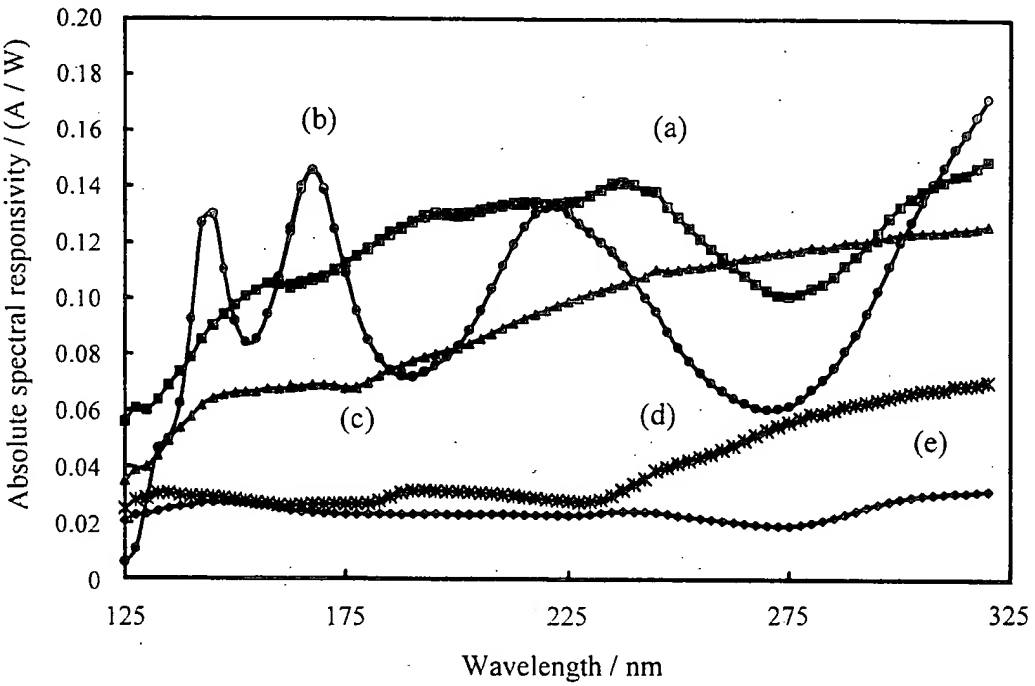

Figure 5. Measured responsivities for various UV detectors: (a) Hamamatsu 5227; (b) IRD UVG (nitrided oxide/Si); (c) GaN; (d) GaP; (e) PtSi.

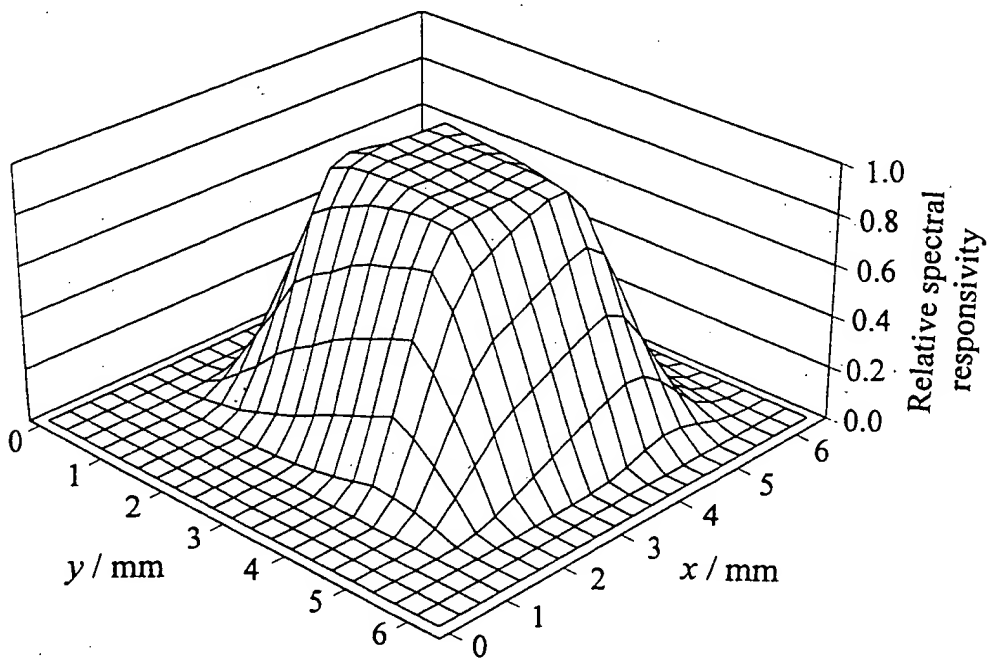

Figure 6. Three-dimensional representation of uniformity (at 180 nm) for a GaN photodiode. The data were obtained by computer-controlled manipulation of translation stages.

As part of the calibration process, the spatial uniformity is also measured by rastering the photodiode in the synchrotron-radiation beam (with slit widths less than 1 mm) and recording the signal at a given wavelength versus the position of the translation stages (see above). Figure 6 is a uniformity scan of a GaN diode at 180 nm.

6. Conclusion

We have constructed a new radiometric beamline at SURF II to measure absolute responsivities of detectors from about 125 nm to 320 nm using an ACR. Along with the results discussed above, we have also measured reflectance, transmittance, and photodiode response to

UV-induced damage. We will discuss these results and the uncertainty analysis for the present results in a separate publication. SURF II is now undergoing a major upgrade (to SURF III). We are also improving the UV radiometry (beamline 4) by using a windowless beamline and better gratings to allow us to go further into the ranges of the UV and visible spectra.

References

1. Schwinger J., *Phys. Rev.*, 1949, **75**, 1912-1925.
2. Furst M. L., Graves R. M., Canfield L. R., Vest R. E., *Rev. Sci. Instrum.*, 1995, **66**, 2257-2259.
3. Cromer C. L., Lucatorto T. B., O'Brian T. R., Walhout M., *Solid State Technology*, April 1996, 75-80.
4. Martin J. E., Fox N. P., Key P. G., *Metrologia*, 1985, **21**, 147-156.
5. Gentile T. R., Houston J. M., Cromer C. L., *Appl. Opt.*, 1996, **35**, 4392-4403.
6. Lau-Frambs A., Kroth U., Rabus H., Tegeler E., Ulm G., Wende B., *Metrologia*, 1995/96, **32**, 571-574.
7. Rabus H., Persch V., Ulm G., *Appl. Opt.*, 1997, **36**, 5421-5440.
8. Rabus H., Scholze F., Thornagel R., Ulm G., *Nucl. Instrum. Meth. in Phys. Res. A*, 1996, **377**, 209-216.
9. Canfield L. R., *Appl. Opt.*, 1987, **26**, 3831-3837.
10. Vest R. E., Canfield L. R., Furst M. L., Madden R. P., Swanson N., *Nucl. Instrum. Meth. in Phys. Res. A*, 1994, **347**, 291-294.
11. Larason T. C., Bruce S. S., Cromer C. L., *J. Res. Nat. Inst. Stand. Tech.*, 1996, **101**, 133-140.
12. Larason T. C., Bruce S. S., Parr A. C., *NIST Spec. Publ.*, 1997, 250-41.
13. Ederer D. L., Cole B. E., West J. B., *Nucl. Instrum. Meth.*, 1980, **172**, 185-190.
14. Hughey L. R., *Nucl. Instrum. Meth. in Phys. Res. A*, 1994, **347**, 294-298.
15. Solt K., Melchior H., Kroth U., Kuschnerus P., Persch V., Rabus H., Richter M., Ulm G., *Appl. Phys. Lett.*, 1996, **69**, 3662-3664.